Int. J. Advanced Design and Manufacturing Technology, 2022, Vol. 15, No. 4, pp. 61-70

DOI: 10.30486/admt.2023.1960408.1355 ISSN: 2252-0406 https://admt.isfahan.iau.ir

Experimental Analysis of Effective Parameters on the Bowing Defect of Symmetrical U-Section in Roll Forming Production

Amin Poursafar, Saeid Saberi *, Rasoul Tarkesh Esfahani, Meisam Vahabi, Javad Jafari Fesharaki

Department of Mechanical Engineering, Najafabad Branch, Islamic Azad University, Najafabad, Iran.
E-mail: amin.poursafar@smc.iaun.ac.ir, saeid_saberi@yahoo.com, ra_tarkesh@pmc.iaun.ac.ir, m.vahabi@pmc.iaun.ac.ir, jafari@pmc.iaun.ac.ir
*Corresponding author

Received: 6 June 2022, Revised: 29 September 2022, Accepted: 23 October 2022

Abstract: The roll forming process plays a critical role in producing various sections used in industries. Also, the quality of these products is strongly affected by the thickness of the strip, the distance between stands, the section web, the flower pattern, and the plastic anisotropy. Therefore, the influences of practical factors on the bowing defect of the symmetrical U-section are experimentally and mathematically characterized in the present research. The investigated material is DC03 (1.0347) steel. Different prediction models such as linear and non-linear model based on the general full-factorial design of experiment are used to predict the effect of following factors on the bowing defect. Accuracy of the analytical model was verified by comparing the output results with the practical data. Results show that the strip thickness of investigated material, the flower pattern, and the section web have the most significant effect on the bowing defect. Also, the anisotropic properties of the investigated material and the inter distance have the minor impact on the bowing defect, but the effect of material with considering the anisotropic properties on increasing the accuracy of process simulation results is very impressive and increases the accuracy of simulation results from 84% to 91%. Finally, the predicted bowing defect using the modified two-factor model was in 91% agreement with the experimental results.

Keywords: Bowing Defect, Design Of Experiments, Full Factorial, Roll Forming, Symmetrical, U- Section

Biographical notes: Amin Poursafar received his MSc in Mechanical Engineering from Urmia university, in 2006 and he is now a PhD student in Mechanical Engineering at IAU, Najafabad branch. His research interest is metal forming and machining**. Saeid Saberi** received his PhD and MSc in Mechanical Engineering from Graz University of Technology, in 2004 and 2009. His research interests include machine visioning, forming processes, and modern production. **Rasoul Tarkesh Esfahani** received his PhD and MSc from Kashan University in 2004 and 2009, respectively. His research interests include solving the challenges of the aviation industry. **Meisam Vahabi** received his PhD and MSc in Mechanical Engineering from Amirkabir University of Technology, in 2004 and 2010, respectively. His research interests include smart material, gear box design, optimizing, tool design, and MEMS. **Javad Jafari Fesharaki** received his PhD, MSc and BSc in Mechanical Engineering from Kashan University, in 2004, 2008 and 2010, respectively. His research interests include functionally graded material, and piezoelectric patch.

Research paper

1 INTRODUCTION

The roll forming process consists of several forming stands with the various forming rolls where the strip with different materials, such as steel, and non-steel, approaches the final geometry at several stands. The stand of the roll forming process consists of a combination of various rollers that create a flower pattern of the profile, and these stands consist of a set of upper and lower rollers for this purpose. Side rollers are used to prevent strip misalignment to improve the forming conditions. One of the most significant advantages of this process is that the thickness does not change during the process. All these features allow to product the various sections with a uniform cross-section longitudinally with the best quality. The most essential features of this type of forming process that has made the overall process uniform is that the power used in all stands is the same.

In this process, the velocity gradient in each stand, which is along with increasing the diameter of the rollers, prevents the sheet from wrinkling. This issue is critical in the case of low-thickness strips, because in the case of thicker strips, wrinkling and bowing defect occur less frequently [1]. Generally, the strip is continuously formed at ambient temperature into a desired cross-section (open or close section) through the forming rolls [2]. Figure 1 shows the schematic of process and the bowing defect; According to "Fig. 1", the bowing defect is accrued in the perpendicular direction to the formed section axes.

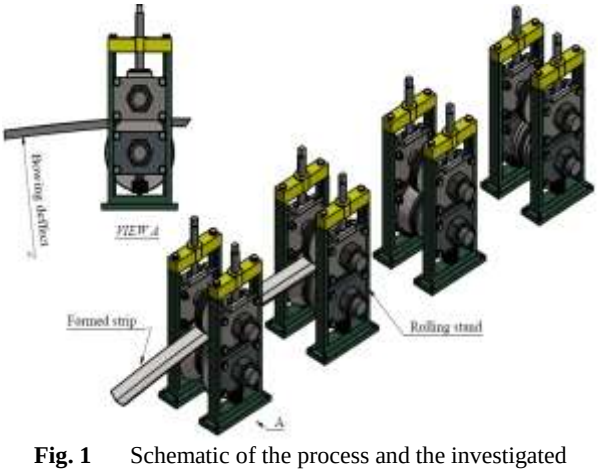

Fig. 1 Schematic of the process and the investigated bowing defect.

It was shown that the bowing defect could be reduced as much as possible by changing the relative height of the rollers of each stand concerning each other, as well as using extra rolls called straighter at the end of the production line [3]. Bhattacharyya et al. showed that the distance between the stands in a roll forming could be significant on the bowing defect. Also, the results of their research show the impact of the thickness, the flower pattern, and the wall length on the bowing defect [4]. Bhattacharyya et al. studied on the effects of the flower pattern on the strains which accrues along with longitudinal direction, and their results showed that the effect of the start and the final forming stands are greater than other stands [5]. Duncan and Zhou investigated the parameters affecting the symmetric part of the U-channel and the hat-shaped section in the multi-stand process. The results of their research revealed the transverse, the longitudinal, and the shear strains as significant factors [6]. By using five sets of rolling stand and choosing a symmetrical section, Sheu found the significant impact of the flower pattern, the velocity of rolls, the friction, and the rolls radius on the bowing defect. The results showed that the velocity and the flower pattern have the greatest effect [7]. Tehrani et al. used ABAQUS software and used the localized buckling at the edge of formed strip as a constraining factor in the roll forming of the symmetrical section of the U-channel. Investigation showed that the amount of bending in the first forming stand should be optimized to prevent the localized edge buckling [8]. Shirani et al. investigated the effects of different on-line factors on the bowing defect of the pre-punched symmetrical U-shaped section. In this study, the stand level height, the bend angle of increment (flower pattern), and the distance between forming stands are considered as input factors, and the circularity of punched-holes after forming took as the result. Finally, the thickness of the strip is presented as the most effective factor on the holes circularity [9]. Shirani et al. also investigated the bowing defect of the U-section product. They investigated different factors like the thickness, the side length, and the flower pattern on the bowing defect and conducted a series of practical tests and verified the results with the ABAQUS software results. The results showed that the thickness and the flower pattern have the greatest effect on the bowing defect of the pre-punched strip [10]. Shirani et al. continued to investigate the effective factors on the torque of the forming stand. Their results showed that increasing the bending angle in each stand increased the required torque, and the torque also moves up with increases in the thickness [11]. Lindgren studied on alloy steel, especially high-strength for producing the symmetrical channel. The longitudinal strain of the formed strip edge decreased with the increase in the inter distance [12]. Salmani et al. predicted the bowing defect using regression models and artificial neural networks. The results of this research show that the regression prediction model and the artificial neural network model are suitable for predicting the process defects [13]. The simulation was performed based on METAFOR software code by Bui for symmetrical U-shaped sections. The results show that the distance of stands, the forming velocity, the friction between the rollers, the

mechanical properties of the strip, and the strip are effective on the longitudinal strains [14]. Lindgren et al. presented a full factorial-based model that the flower pattern was considered as an input factor. The results of this research show that the section web and the flower pattern significantly affect the length of deformation needed for forming at each stand. Also, the strain of the strip has shown a significant increase with increasing the strip thickness [15]. Zeng et al. investigated the U-channel section using 3D finite element analysis by ABAQUS software. In this research, a statistical relationship for roller design is presented. In this research, by using four-factor models between the flower pattern and the spring back, the number of forming stands was reduced [16]. Punin et al. investigated the reduction of the bowing defect by considering the forming stand. The distance between forming stands, the flower pattern, and the thickness have the greatest effect on the bowing defect [17]. Cha et al. investigated the effect of strains along the forming direction on the final geometry of the product. In this research, high-strength steel was selected, and by creating additional pressure on the sheet along the thickness, the effects of the bowing defect were significantly reduced [18]. Wiebenga et al. studied the bowing defect and the spring-back on a V-shaped channel, and by optimizing the inter distance, product defects were reduced [19]. Safdarian et al. investigated the impact of different factors on the bowing defect and the strains on the roll forming process. The results indicated that increase in the flower pattern and the thickness of the strip increase the strain in the forming direction [20]. Shirani et al. studied on the over-bending defects. The results showed that this defect could be decreased by decreasing the flower pattern [21]. Heydari et al. worked on accumulative roll bonding (ARB) to produce especial composites. The results indicated that mechanical properties of samples improved with increasing the temperature of ARB cycles. But in ambient temperature, ARB cycles, the sample toughness and the sample elongation decreased [22]. Heydari et al. also worked on the asymmetric roll bonding process. They used ABAQUS software to model the deformation of samples. The results showed that increasing the strain at the bimetal interface leads to improvement of the bonding quality [23]. Sattar et al. worked on a special notched U-section in the cold forming production. The results indicated that with increasing the diameter of punched holes, the buckling of the section wall increases [24].

The impact of the anisotropic properties on the bowing defect was not investigated. The costs of designing and manufacturing forming rollers for manufacturers of roll forming products show that providing accurate simulation models with the ability to estimate the final shape of the product is very important. Therefore, in this research, a finite element model considering the impact of material properties especially definition of anisotropic properties on the bowing defect of the product was investigated with 91% accuracy using a linear and non-linear numerical model along with simulation in ABAQUS software.

2 MATERIAL AND METHODS

The target product which is selected was a special basic U-section with a 45° bend angle on side walls. The schematic characteristics of the selected section are presented in “Fig. 2”.

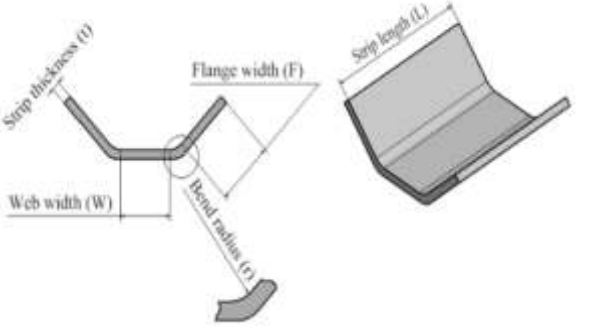

Fig. 2 Characteristics of the investigated U-channel section.

The DC03 (1.0347) steel is used for this study. This type of steel is common and widely used in the structural and construction industry. The engineering stress-strain curve of investigated steel was obtained using the procedure according to ASTM E8 standard. The result of test for DC03 steel in two different directions is presented in “Fig. 3”.

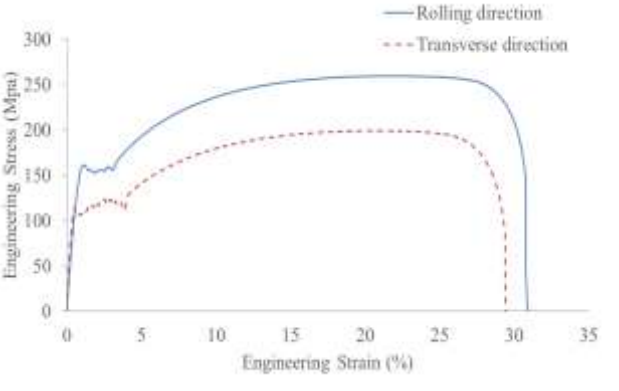

Fig. 3 The engineering stress-strain curve for 1.0347 steel

To analyses, the anisotropy, half of the samples were re-annealed to be made isotropic properties. The mechanical properties of the strips are presented in “Table 1”.

Table 1 Mechanical and mass density of the investigated material

Elastic modulus (Mpa)	207000
Poisson ratio	0.3
Elastic strain limitation	0.002
Density (Kg/m³)	7800
Elongation (%)	45
Yield (Mpa)	
Thk. =2 (mm)	213
Thk. =2.5 (mm)	210

"Table 2" shows the investigated affected values studied in this research. These values are considered with the capabilities of the roll forming apparatus used to perform practical tests.

Table 2 levels of input factors for the investigated design of experiment

Factor	Values	
Flower pattern (angle increment)	□15	□22.5
Section web(w)	40 mm	20 mm
Thickness (t)	2.5 mm	2 mm
Distance between stands(d)	500 mm	300 mm
Structure condition (H)	Re-Annealed	Anisotropic

The complete data of experiments and simulations are presented in "Table 3".

Table 3 The complete data of experiments and simulations

Test No.	Structure condition	Thickness mm	Width of section, mm	Angle increment, degree	Distance between stands, mm	Simulation bowing defect, mm	Experimental bowing defect, mm
1	Iso	2	20	22.5	500	5.62	9.37
2	Iso	2.5	40	22.5	500	7.23	10.04
3	Aniso	2.5	20	15	500	25.63	12.26
4	Aniso	2	20	15	300	7.40	7.50
5	Aniso	2	20	15	500	1.97	5.24
6	Iso	2.5	20	15	500	23.61	32.59
7	Aniso	2	20	22.5	300	8.87	20.12
8	Iso	2.5	40	15	300	24.84	22.60
9	Iso	2.5	20	15	300	4.09	7.39
10	Aniso	2	40	22.5	500	2.10	5.56
11	Iso	2	40	15	300	12.42	15.67
12	Iso	2	40	15	500	10.74	15.23
13	Aniso	2.5	40	22.5	300	12.88	13.42
14	Aniso	2.5	40	15	300	28.86	42.08
15	Aniso	2.5	20	15	300	5.53	22.30
16	Iso	2.5	40	15	500	33.14	42.65
17	Iso	2	20	15	300	10.66	19.76
18	Iso	2.5	20	22.5	500	13.82	16.80
19	Iso	2	40	22.5	300	1.89	6.89
20	Aniso	2	40	22.5	300	1.89	6.58
21	Aniso	2	20	22.5	500	4.39	8.35
22	Iso	2	20	22.5	300	10.90	16.32
23	Aniso	2.5	20	22.5	500	14.72	16.68
24	Iso	2.5	40	22.5	300	9.18	7.65
25	Iso	2	40	22.5	500	2.13	2.65
26	Iso	2	20	15	500	3.56	6.11
27	Aniso	2	40	15	300	11.34	16.55
28	Aniso	2.5	40	15	500	35.86	23.56
29	Iso	2.5	20	22.5	300	13.25	19.20
30	Aniso	2	40	15	500	11.46	12.03
31	Aniso	2.5	20	22.5	300	14.62	16.65
32	Aniso	2.5	40	22.5	500	7.29	12.68

Aniso=Anisotropic
Iso=Isotropic(Re-Annealed)

The investigated roll forming machine includes a 45-kilo-watt motor supplier with the ability to transmit power to seven forming stands. The device is equipped with a precise speed adjustment unit, precise sets of gearboxes, and set of guide rolls were also used to prevent the movement of the pre-formed strip in the side direction. Figure 4 shows the roll forming apparatus which are used for practical tests.

Fig. 4 Roll forming apparatus of the investigated machine.

The forming speed process was determined to be 22 mm/sec according to the precise control conditions of practical tests. Forming rolls are combined into two pieces. The flat disc (B) was used to perform different section webs, and the angled rolls (A) were used to perform bending angles. Figure 5 shows the assembly of the disc and the bending rolls.

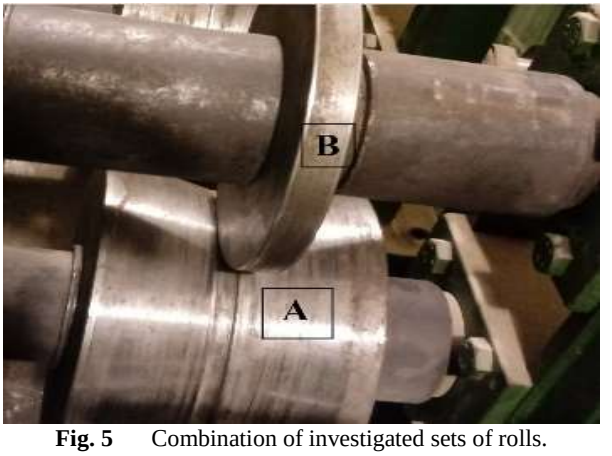

Fig. 5 Combination of investigated sets of rolls.

National Instruments Vision Software with 12-megapixel camera have been used to measure the defect of samples; In this measurement method, the difference between the end points position of the sample and the mid-position of it was measured as bowing defect according to "Fig. 6".

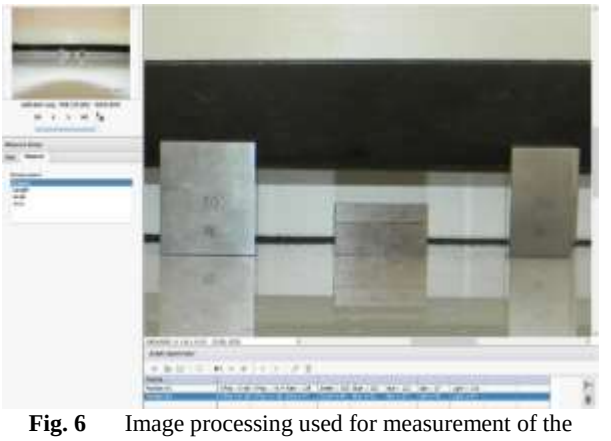

Fig. 6 Image processing used for measurement of the bowing defect.

The gauge block was used to convert the Acquisition data to dimension. To reduce the measurement error in this method, the measurements were performed in three stages for the rolled samples, and the average of the obtained measurements was considered the bowing defect.

3 PROCESS SIMULATION

The finite element simulation modelling of the roll forming was performed in ABAQUS software; the investigated model is shown in "Fig. 7".

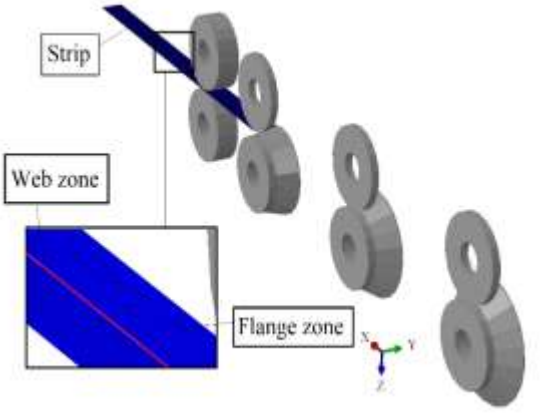

Fig. 7 Finite element model and the mesh zone detail.

The model includes the sheet strip and forming rolls with the same dimension as the rolls used in the practical tests. In the examined model, the forming rolls were defined as an analytical rigid part, and the sheet strip was designed as a shell part. To measure the longitudinal strain, a path was created on the edge and, the bottom of the samples, which is called the flange path and the web path. The distribution of the strain along the rolling direction is presented in "Fig. 8".

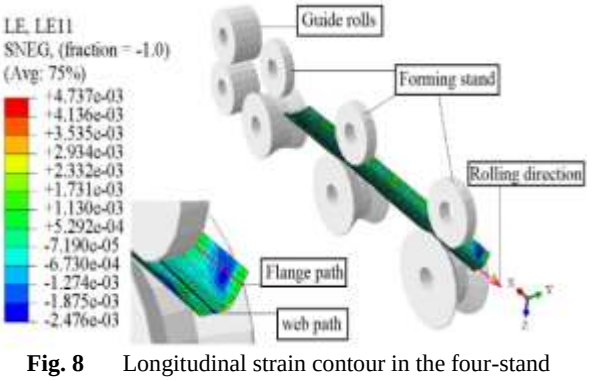

Fig. 8 Longitudinal strain contour in the four-stand forming simulation.

To obtain the optimized distribution of meshes, two different zones were defined for meshing, which is

presented in "Fig. 7". Considering that the sheet strip is defined as a shell type, S4R element used for shell type parts with five points for integration in the direction of the thickness were selected [8]. To define the friction condition between the forming rolls and the sheet strip, a penalty coefficient of 0.2 was considered. The gap size in all forming stands was considered according to the thickness of the sheet strip. To model the strip for both non-homogeneous and homogeneous states, anisotropy properties were assessed using the Hill 48 equation and calculated R-values coefficient. Since the raw material is affected by the rolling production conditions, and according to "Fig. 3", the mechanical properties of it were different in rolling and transverse directions. Hill introduced a yield criterion, which is given in "Eq. (1)" [25].

$$2f = F(\sigma_{22} - \sigma_{33})^2 + G(\sigma_{33} - \sigma_{11})^2 + H(\sigma_{11} - \sigma_{22})^2 + 2L{\sigma_{23}}^2 + 2M{\sigma_{31}}^2 + 2N{\sigma_{12}}^2 \quad (1)$$

In "Eq. (1)", f is the Hill yield function, and the material constants are defined with F, G, H, L, M, and N. Six yield strain ratios r_{11}, r_{22}, r_{33}, r_{12}, r_{13}, and r_{23} are calculated according to "Eq. (6), Eq. (7), Eq. (8), and Eq. (9)". The plane strain condition eliminated the L and M constants from "Eq. (1)" [25]. To determine the coefficients, the standard test of the samples was performed according to ASTM E8. According to this standard, the measurements of the strain ratio in three rolling, transverse, and thickness directions were performed using special strain gauges; the coefficients were calculated according to "Eq. (2) to Eq. (9)". The obtained plastic strains ratio (r_{xy}) or Lankford coefficients from the specified test are shown in "Table 4". In "Table 4", the number 1 is rolling direction and 2 is transverse direction and 3 is thickness direction.

$$F = \frac{1}{2}\left(\frac{1}{{r_{22}}^2} + \frac{1}{{r_{33}}^2} - \frac{1}{{r_{11}}^2}\right) \quad (2)$$

$$G = \frac{1}{2}\left(\frac{1}{{r_{33}}^2} + \frac{1}{{r_{11}}^2} - \frac{1}{{r_{22}}^2}\right) \quad (3)$$

$$H = \frac{1}{2}\left(\frac{1}{{r_{11}}^2} + \frac{1}{{r_{22}}^2} - \frac{1}{{r_{33}}^2}\right) \quad (4)$$

$$N = \frac{3}{2r_{12}^2} \quad (5)$$

$$r_{11} = r_{13} = r_{23} = 1 \quad (6)$$

$$r_{22} = \sqrt{\frac{r_{90}(r_0+1)}{r_0(r_{90}+1)}} \quad (7)$$

$$r_{33} = \sqrt{\frac{r_{90}(r_0+1)}{(r_{90}+r_0)}} \quad (8)$$

$$r_{12} = \sqrt{\frac{3r_{90}(r_0+1)}{(2r_{45}+1)(r_{90}+r_0)}} \quad (9)$$

Table 3 Calculated R-values of the investigated material

Test No.	r_{22}	r_{33}	r_{12}
1	1.026	1.293	5.112
2	1.018	1.25	5.23
3	1.015	1.307	5.025
r_{11}, r_{13}, r_{23}	1		

4 RESULTS

Investigation of different input factors on the bowing defects was done using design expert software. The analytical model was obtained from the full-factorial design of experiment. Examination and analysis of the simulation results and experiments illustrated the robustness of the analysis and results. "Table 5" shows the complete data of variance analysis of the investigated model.

Table 4 Variance analysis of complete data for modified two-factor model

Factor	Sum of squares	DOF	Mean square	F-value	P-value
Model	2359.2	11	214.5	13.8	< 0.0001
A-Structure condition	1.86	1	1.86	0.12	0.7327
B-Thickness	873.66	1	873.7	56.3	< 0.0001
C-Section web	62.16	1	62.16	4.01	0.059
D-Flower pattern	452.31	1	452.3	29.2	< 0.0001
E-Distance between stands	18.98	1	18.98	1.22	0.2818
AB	19.08	1	19.08	1.23	0.2805
BC	58.94	1	58.94	3.8	0.0654
BD	100.78	1	100.8	6.5	0.0191
BE	159.47	1	159.5	10.3	0.0044
CD	510.48	1	510.5	32.9	< 0.0001
DE	101.49	1	101.5	6.54	0.0188
Residual	310.21	20	15.51	-	-
Cor total	2669.4	31	-	-	-

Based on this analysis, if the F-value of variance analysis is large and the root-mean-square is close enough to 1, the model's accuracy can be assured. Considering the F-value and R-square of linear, two-factor, and three-factor fitted models are presented in "Fig. 9", according to F-value of 13.83 and R-square of 0.91, the modified two-factor model is accurate enough for prediction of bowing defect. If P<0.05 for the factors examined in this model, it indicates the effect of that factor on the bowing defect [24]. Figure 9 shows the comparison between F-value and R-square in different states, including linear, two-factor, and three-factor models. Figure 10 illustrates the actual vs. predicted values of the analytical bowing defect model. The density of the data around the central line, and the obtained R-square, proves the correctness of the modified two-factor model.

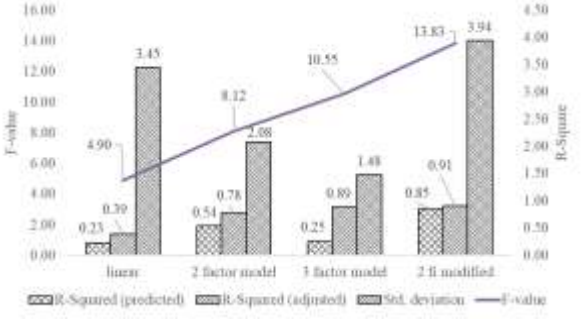

Fig. 9 R-square and F-value for investigated models.

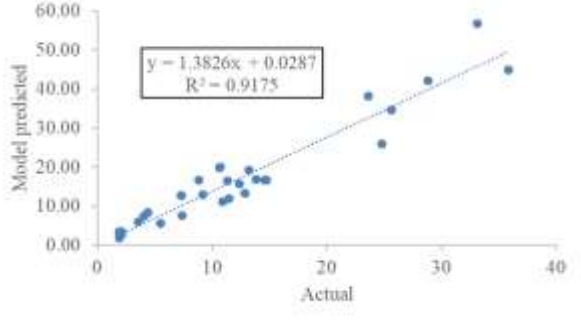

Fig. 10 Comparing actual and model predictions of the bowing defect.

According to the results of the model, it can be seen that the bowing defect is increased with increases in the thickness. According to "Eq. (10)", increasing the thickness reduces the length of the deformation when the strips enter the forming stand, and according to "Eq. (11)", it increases the longitudinal strain [26].

$$L = \sqrt{\frac{8a^3\theta}{3t}} \tag{10}$$

$$\varepsilon = \sqrt{1 + 2\left(\frac{a}{L}\right)^2 (1 - cos\,\theta)} - 1 \tag{11}$$

All the parameters used in "Eq. (10) and Eq. (11)" are shown in "Fig. 11". Considering the fix value for the angle at each stand (θ) and the wall length of section (a), the length for the roll forming process at each stand (L) is decreased with increasing the thickness.

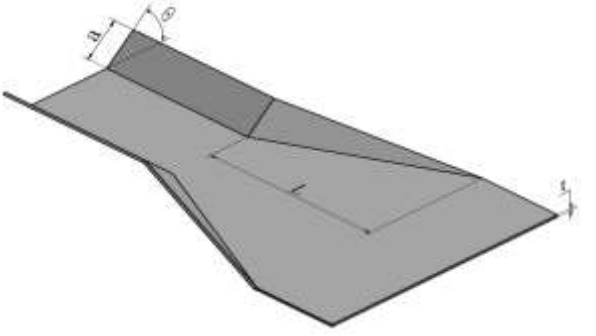

Fig. 11 Significant parameters of forming process.

The effect of the thickness on the bowing defect both in the experimental and the simulation is presented in "Fig. 12". As it is shown in "Fig. 12" with increasing the thickness the bowing defect is increased.

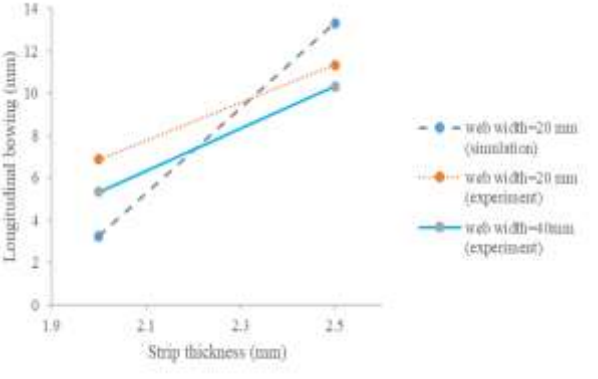

Fig. 12 Effect of the thickness on the bowing defect in experiment and simulation.

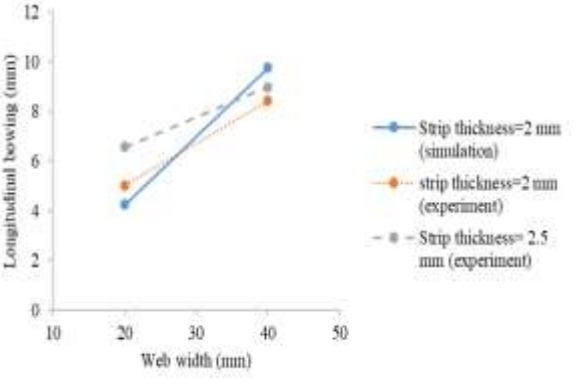

Fig. 13 Effect of section web on the bowing defect in experiment and simulation.

The effect of the section web on the bowing defect is presented in "Fig. 13". Accordingly, expanding the section web increases the bowing defect. Increasing the section web reduces the bending resistance during bending, and then increases the bowing defect of the product. In addition, with considering to "Eq. (10)", expanding the wall length of section (a) increases the strip length that enter the stands [27]. The effect of the stand longitudinal distance on the bowing defect is shown in "Fig. 14". As it is shown, with increasing the stand longitudinal distance, the bowing defect of the sample is decreased. Also, according to "Fig. 15", with decreasing the flower pattern, the bowing defect can be decreased. It can be resulted that reducing the flower pattern minimizes the strains difference between the section wall and the section web, so the bowing defect is reduced [26].

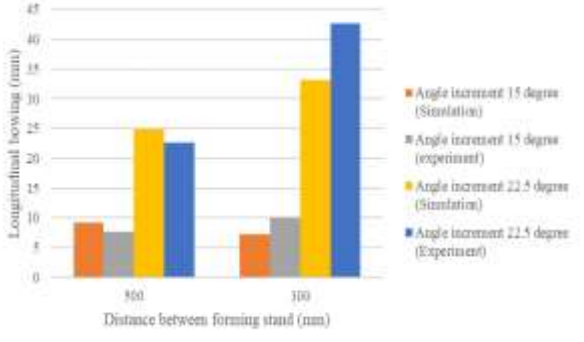

Fig. 14 Effect of the stand longitudinal distance on the bowing defect in experiment and simulation.

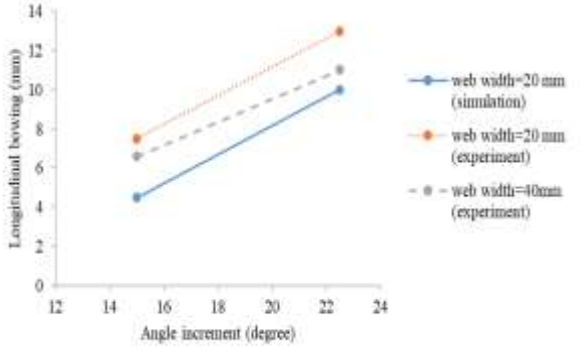

Fig. 15 Effect of the angle incrementation on the bowing defect in experiment and simulation.

As shown in "Fig. 14 and Fig. 15", the bowing defect was decreased with reducing the flower pattern increment. Also, with reduction of the section web dimension, the bowing defect decreases more. According to "Fig. 16", both the results of experiments and the results of simulations show the insignificant impact of the structure condition on the bowing defect, but anisotropic or isotropic properties have a significant impact on the consequences of finite elements results, and the accuracy of the model has increased from 84% to 91%.

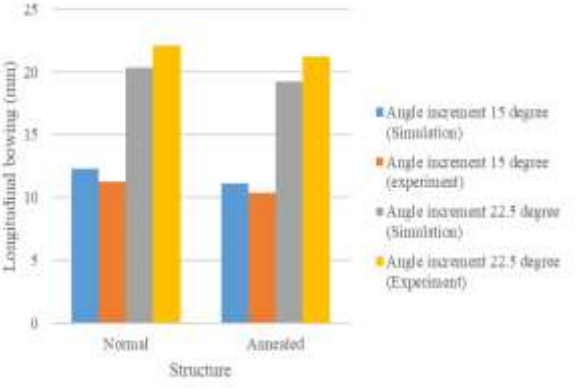

Fig. 16 Effect of structure on the bowing defect.

This result proves that the coefficient of anisotropic properties should be considered in definition of strip material properties for the simulation model. The comparison of the simulation results vs. practical tests is presented in "Fig. 17".

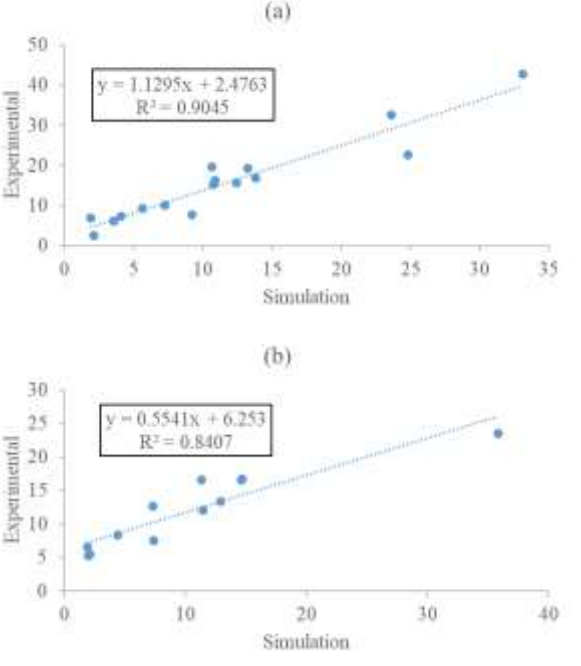

Fig. 17 Simulation vs. experimental values of bowing defect: (a): with anisotropy consideration, and (b): Without anisotropy consideration.

The analytical models, based on both experimental results and the simulation data, were presented in "Fig. 9". Also, the modified two-level of influential factors are analyzed. By checking the R-square value obtained from the analytical model (91%), the accuracy of the model could be confirmed. P-value, which was mentioned

before, shows the impact of the investigated factor on the bowing defect. The low value of this coefficient expresses the intensity of the parameter on the bowing defect. Equation (12) shows the analytical model where A is the structure condition, B is the thickness, C is the width of the section, D is the flower pattern, and E is the distance between stands.

$$Bowing = 11.93 + 0.24A + 5.23B + 1.39C - 3.76D + 0.77E + 0.77AB + 1.36BC + 1.77BD + 2.23BE - 3.99CD - 1.78DE \quad (12)$$

The accuracy of the modified two-factor analytical model values is presented in "Table 6". The coefficient of variation is calculated from "Eq. (13)" [27]. In "Eq. (13)", S_{dev} is standard deviation and M is the mean values, which are calculated from the selected model according to "Table 6".

$$Coefficient\ of\ variation(\%) = \frac{S_{dev}}{M} \times 100 \quad (13)$$

Table 5 Accuracy of the selected analytical model on the bowing defect

Model	R^2 adjusted	Standard deviation	Mean	C.V. %
Modified Two factors	0.91	3.94	11.93	33

Figure 18 shows the Pareto chart of the investigated factors on the bowing defect. The strip thickness has the most remarkable effect and anisotropy properties has the most minor impact on the bowing defect. Also, the flower pattern effect on the bowing defect is significant.

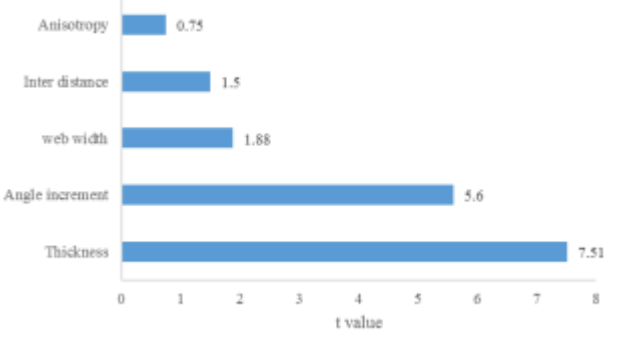

Fig. 18 The impact severity of the investigated parameters on the bowing defect.

5 CONCLUSION

The results of the current research show the effects of the parameters listed in "Table 2" on the bowing defect as follows:

- The thickness of the strip is the most influential factor in the bowing defect of symmetrical U-shaped channels. The bowing defect is directly related to sheet thickness. In other words, with the constant value of the flower pattern and the section web, increasing the thickness reduces the required strip length at each stand of the forming process, followed by an increase in bowing defect.
- The flower pattern influences the bowing defect as a second influential factor. Reducing the angle increment change in each stand reduces the bowing defect. It should be noted that the reduction of angle increment in each stand means an increase in the number of forming stands, which can lead to an increase in the cost of making rollers to create more stands, which makes choosing the optimal value for the flower pattern very essential. The optimal value is considered 15-degree incrementation.
- The section web is another significant parameter in the bowing defect of symmetrical U-shaped channels. By reducing the cross-section web, the difference in generated strain between the section wall and the web area is reduced, and reduces the bowing defect. The distance between stands does not have significant impact on the bowing defect of symmetrical U-shaped channels.
- Plastic anisotropy has a significant impact on the results of finite element simulation, and the accuracy of the simulation has increased from 84% to 91%.
- The analytical models, based on both experimental results and the simulation data, showed that the modified two-level model has the reasonable R-square value (91%) and the accuracy of the model could be confirmed.

REFERENCES

[1]Halmos, G. T., Roll Forming Handbook, 2005. DOI: 10.1201/9781420030693.

[2]Shirani Bidabadi, B., Moslemi Naeini, H., Azizi Tafti, R., and Barghikar, H., Experimental Study of Bowing Defects in Pre-Notched Channel Section Products in The Cold Roll Forming Processint, J. Adv. Manuf. Technol., Vol. 87, No. 1–4, 2016, pp. 997–1011, DOI: 10.1007/s00170-016-8547-y.

[3]Ona, H., Experiments into the Cold Roll Forming of Straight Asymmetrical Channels, J. Mech. Work. Technol., Vol. 8, No. 83, 1983, pp. 273–291.

[4]Bhattacharyya, D., Smith, P. D., Thadakamalla, S. K., and Collins, I. F., The Prediction of Roll Load in Cold Roll-Forming, J. Mech. Work. Technol., Vol. 14, No. 3, 1987, pp. 363–379, DOI: 10.1016/0378-3804(87)90019-2.

[5]Bhattacharyya, D., Smith, P. D., The Development of Longitudinal Strain in Cold Roll Forming and Its Influence

on Product Straightness, leAdv. Technol. Plast., Vol. 1, 1984, pp. 422–427.

[6]Panton, S., Duncan, J., and Zhu, S., Longitudinal and Shear Strain Development in Cold Roll Forming, J. Mater. Process. Technol., Vol. 60, 1996, pp. 219–224, DOI: 10.1016/0924-0136(96)02333-3.

[7]Sheu, J. J., Simulation and Optimization of The Cold Roll-Forming Process AIP Conf. Proc., Vol. 1, 2004, pp. 452–457, DOI: 10.1063/1.1766566.

[8]Tehrani, M. S., Hartley, P., Naeini, H. M., and Khademizadeh, H., Localised Edge Buckling in Cold Roll-Forming of Symmetric Channel Section Thin-Walled Struct., Vol. 44, No. 2, 2006, pp. 184–196, DOI: 10.1016/j.tws.2006.01.008.

[9]Shirani Bidabadi, B., Moslemi Naeini, H., Azizi Tafti, R., and Mazdak, S., Experimental Investigation of The Ovality of Holes on Pre-Notched Channel Products in The Cold Roll Forming Process, J. Mater. Process. Technol., Vol. 225, 2015, pp. 213–220, DOI: 10.1016/j.jmatprotec.2015.06.008.

[10] Shirani Bidabadi, B., Moslemi Naeini, H., Salmani Tehrani, M., and Barghikar, H., Experimental and Numerical Study of Bowing Defects in Cold Roll-Formed, U-Channel Sections, J. Constr. Steel Res., Vol. 118, 2016, pp. 243–253, DOI: 10.1016/j.jcsr.2015.11.007.

[11] Shirani Bidabadi, B., Moslemi Naeini, H., Azizi Tafti, R., and Tajik, Y., Optimization of Required Torque and Energy Consumption in The Roll Forming Process, Int. J. Interact. Des. Manuf., Vol. 13, No. 3, 2019, pp. 1029–1048, DOI: 10.1007/s12008-019-00564-9.

[12] Lindgren, M., Cold Roll Forming of a U-Channel Made of High Strength Steel, J. Mater. Process. Technol., Vol. 186, No. 1–3, 2007, pp. 77–81, DOI: 10.1016/j.jmatprotec.2006.12.017.

[13] Poursina, M., Salmani Tehrani, M., and Poursina, D., Application of BPANN and Regression for Prediction of Bowing Defect in Roll-Forming of Symmetric Channel Section, Int. J. Mater. Form., Vol. 1, No. 1, 2008, pp. 17–20, DOI: 10.1007/s12289-008-0057-5.

[14] Bui, Q. V., Ponthot, J. P., Numerical Simulation of Cold Roll-Forming Processes, J. Mater. Process. Technol., Vol. 202, No. 1–3, 2008, pp. 275–282, DOI: 10.1016/j.jmatprotec.2007.08.073.

[15] Lindgren, M., An Improved Model for The Longitudinal Peak Strain in The Flange of a Roll Formed U-Channel Developed by FE-Analyses Steel Res. Int., Vol. 78, No. 1, 2007, pp. 82–87, DOI: 10.1002/srin.200705863.

[16] Wei Zhang, H., Zhong Liu, L., Hu, P., and Hua Liu, X., Numerical Simulation and Experimental Investigation of Springback in U-Channel Forming of Tailor Rolled Blank, J. Iron Steel Res. Int., Vol. 19, No. 9, 2012, pp. 8–12, DOI: 10.1016/S1006-706X(13)60002-3.

[17] Punin, V. I., Kokhan, L. S., and Morozov, Y. A., Reduction of the Length of Strip Rolled on Roll-Forming Machines Metallurgist, Vol. 56, No. 11–12, 2013, pp. 938–940, DOI: 10.1007/s11015-013-9678-0.

[18] Gi Cha, W., Kim, N., Study on Twisting and Bowing of Roll Formed Products Made of High Strength Steel, Int. J. Precis. Eng. Manuf., Vol. 14, No. 9, 2013, pp. 1527–1533, DOI: 10.1007/s12541-013-0206-8.

[19] Wiebenga, J. H., Weiss, M., Rolfe, B., and Van Den Boogaard, A. H., Product Defect Compensation by Robust Optimization of a Cold Roll Forming Process, J. Mater. Process. Technol., Vol. 213, No. 6, 2013, pp. 978–986, DOI: 10.1016/j.jmatprotec.2013.01.006.

[20] Safdarian, R., Moslemi Naeini, H.,The Effects of Forming Parameters on The Cold Roll Forming of Channel Section Thin-Walled Struct., Vol. 92, 2015, pp. 130–136, DOI: 10.1016/j.tws.2015.03.002.

[21] Shirani Bidabadi, B., Moslemi Naeini, H., Safdarian, R., and Barghikar, H., Investigation of Over-Bending Defect in The Cold Roll Forming of U-Channel Section Using Experimental and Numerical Methods, Proc. Inst. Mech. Eng. Part B J. Eng. Manuf., Vol. 236, No. 10, 2022, pp. 1380–1392, DOI: 10.1177/09544054221076628.

[22] Heydari Vini, M., Farhadipour, P., Fabrication of AA1060/Al2O3 Composites by Warm Accumulative Roll Bonding Process and Investigation of its Mechanical Properties and Microstructural Evolution ADMT J., Vol. 10, No. 4, 2017, pp. 91–98, [Online] Available: https://admt.majlesi.iau.ir/article_537192.html.

[23] Heydari, V. M., Saeed, D., Bonding Evolution of Bimetallic Al/Cu Laminates Fabricated by Asymmetric Roll Bonding, Adv. Mater. Res., Vol. 8, No. 1, 2019, pp. 1–10, DOI: 10.12989/AMR.2019.8.1.001.

[24] Sattar, S., Mazdak, S., and Sharifi, E., Numerical Analysis of Circular Pre-notched U-Channel Section Distortions in Cold Roll-Forming ProcessADMT J., Vol. 10, No. 2, 2017, pp. 121–131, [Online] Available: https://admt.majlesi.iau.ir/article_535020.html.

[25] Hill, R., Orowan, E., A Theory of the Yielding and Plastic Flow of Anisotropic Metals, Proc. R. Soc. London. Ser. A. Math. Phys. Sci., Vol. 193, No. 1033, 1948, pp. 281–297, DOI: 10.1098/rspa.1948.0045.

[26] Han, Z. W., Liu, C., Lu, W. P., and Ren, L. Q., Simulation of a Multi-Stand Roll-Forming Process for Thick Channel Section, J. Mater. Process. Technol., Vol. 127, No. 3, 2002, pp. 382–387, DOI: 10.1016/S0924-0136(02)00411-9.

[27] Mander, S. J., Panton, S. M., Dykes, R. J., and Bhattacharyya, D., Chapter 12 Roll Forming of Sheet Materials, in Composite Sheet Forming, Vol. 11, D. B. T. C. M. S. Bhattacharyya, Ed. Elsevier, 1997, pp. 473–515, DOI: https://doi.org/10.1016/S0927-0108(97)80014-8.